Acta Oceanol. Sin., 2021, Vol. 40, No. 7, P. 119–128
https://doi.org/10.1007/s13131-021-1762-x
http://www.aosocean.com
E-mail: ocean2@hyxb.org.cn

Rapid decrease in Antarctic sea ice in recent years

Guanghua Hao[1], Hui Shen[1], Yongming Sun[2, 3*], Chunhua Li[1]

[1] Key Laboratory of Marine Hazards Forecasting, National Marine Environmental Forecasting Center, Ministry of Natural Resources, Beijing 100081, China

[2] Key Laboratory of Physical Oceanography, College of Oceanic and Atmospheric Sciences, Ocean University of China, Qingdao 266100, China

[3] Pilot National Laboratory for Marine Science and Technology (Qingdao), Qingdao 266237, China

Received 13 October 2020; accepted 13 November 2020

Abstract

A 41-year Antarctic sea ice concentration (SIC) dataset derived from satellite passive microwave radiometers during the period of 1979–2019 has been used to analyze sea ice changes in recent decades. The trends of SIC and sea ice extent (SIE) are calculated during the periods of 1979–2019, 1979–2013, and 2014–2019. The trends show regionally dependent features. The SIC shows an increasing trend in most of the regions except the Bellingshausen Sea and Amundsen Sea (BA) during 1979–2019 and 1979–2013. The SIE trend shows a decreasing or decelerating trend in the period of 1979–2019 ((6 835±2 210) km^2/a) compared with the 1979–2013 period ((18 600±2 203) km^2/a). In recent years (2014–2019), the SIC and SIE have exhibited decreasing trends (–(34 567± 3 521) km^2/month), especially in the Weddell Sea (WS) and Ross Sea (RS) during summer and autumn. The trends are related to regionally dependent causes. The analyses show that the SIC and SIE decreased in response to the warming trend of 2 m air temperature ($T_{\text{a-2m}}$) and have exhibited a good relationship with $T_{\text{a-2m}}$ in summer and autumn in recent years. The sea ice decrease in the Antarctic is mainly caused by increases in absorbed energy and southward energy transportation in recent years, such as the increase in gained solar radiation and moist static energy from the south, which demonstrate notable regional characteristics. In the WS region, the local positive feedback from the additional absorbed solar radiation, resulting in warmer air and reduced sea ice, is the main reason for the sea ice decrease in recent years. The increase in southward energy transport has also favored a decrease in sea ice. In the RS region, the increase in southward-transported moist static energy has contributed to the decrease in sea ice, and the increases in cloud cover and longwave radiation have prevented sea ice growth.

Key words: sea ice, Antarctic, decreasing, atmosphere

Citation: Hao Guanghua, Shen Hui, Sun Yongming, Li Chunhua. 2021. Rapid decrease in Antarctic sea ice in recent years. Acta Oceanologica Sinica, 40(7): 119–128, doi: 10.1007/s13131-021-1762-x

1 Introduction

Sea ice plays an important role in the climate system, hindering the exchange of energy and moisture between the ocean and atmospheric climate through ice albedo feedback (Curry et al., 1995; Elders and Pegion, 2019). Satellite-observed data provide abundant information on Arctic and Antarctic sea ice, including interannual and interdecadal variations, since 1978 (Comiso et al., 2017a, b; Comiso and Nishio, 2008; Cavalieri and Parkinson, 2008). In recent decades, Arctic and Antarctic sea ice changes have shown asymmetric and opposing trend, including rapidly decreases in sea ice extent (SIE) and sea ice area (SIA) in the Arctic, with average rates of –4.36% per decade and –4.57% per decade, respectively, during 1978–2015 (Comiso et al., 2017b).

Unlike the Arctic, which is bordered by the Eurasian continent, Antarctica is surrounded by the ocean. Sea ice is intimately coupled with atmosphere-ocean processes over the Southern Ocean (Lee et al., 2017). Many studies have shown a pronounced increase in Antarctic sea ice in recent decades. Early studies showed that the total Antarctic SIE increased by approximately 14 300 km^2/a during 1979 to 1996, and by 13 800 km^2/a up to 1998 (Cavalieri et al., 1997; Zwally et al., 2002). Liu et al. (2004) found that the sea ice concentration (SIC) in the Pacific sector increased 4%–10% per decade from 1979 to 2012. Parkinson and Cavalieri (2012) show that the SIE increased with a slope of (1.5±0.4)% per decade from 1979 to 2010, increasing from the slope for the shorter period during 1979 to 2006 (Cavalieri and Parkinson, 2008), which also indicates that the positive trend becomes significant over 20–28 years. Antarctic sea ice has shown a positive trend except in the Bellingshausen Sea and Amundsen Sea (BA) region (Yuan et al., 2017). The SIE of the southwestern Pacific Ocean shows no significant trend, and the Weddell Sea (WS), Indian Ocean (IO), and Ross Sea (RS) all have positive trends from 1979 to 2010 (Parkinson and Cavalieri, 2012; Simpkins et al., 2013). The updated results show that the overall SIE trend during the 1979–2015 period is estimated to be 1.7% per decade and is dominantly positive in the RS region but dominantly negative in the BA region (Comiso et al., 2017a).

Previous investigations have reported the impacts of atmospheric and oceanic variability on Antarctic sea ice change; for example, Antarctic sea ice shows an increasing trend under

Foundation item: The National Key R&D Program of China under contract Nos 2018YFA0605902 and 2018YFA0605903; the National Natural Science Foundation of China under contract Nos 41606218 and 41941009; the fund of Chinese National Antarctic Research Expedition logistics support item.

*Corresponding author, E-mail: sym@ouc.edu.cn

warm conditions (Zhang, 2007), which indicates a complicated relationship with surface air temperature (Shu et al., 2012). The Antarctic Peninsula and western Antarctica have been among the most rapidly warming regions on Earth over the past several decades (Bromwich et al., 2013; Nicolas and Bromwich, 2014). Additionally, in recent decades, many results have shown Antarctic sea ice changes with El Niño-Southern Oscillation (ENSO) (Liu et al., 2004) and Southern Annular Mode (SAM) in recent decades (Marshall, 2003; Holland et al., 2017; Cerrone and Fusco, 2018; Doddridge and Marshall, 2017), which are the dominant atmospheric modes in the Southern Hemisphere (Thompson and Wallace, 2000). However, the magnitude of the associated ice changes is much smaller than that of the regional ice trend (Liu et al., 2004), and the SAM explains only approximately one third of the variability (Marshall, 2007).

A recent study with SIE data updated to the end of 2018 shows that the increased SIE trend reversed in 2014, with decreasing rates during 2014–2017 far exceeding the decay rates observed in the Arctic (Parkinson, 2019). This study did not reveal the reasons but discussed sea ice retreat in late 2016. Recent studies show that the sea ice retreat in late 2016 was caused by multiple influences, such as strong northerly atmospheric flow in the WS (Turner et al., 2017), persistent zonal wave 3 atmospheric circulation around Antarctica (Wang et al., 2019; Schlosser et al., 2017; Meehl et al., 2019), an unusually negative SAM (Stuecker et al., 2017), and weakened polar stratospheric vortex in the Indian and Pacific Oceans (Wang et al., 2019). However, sea ice changes related to the ENSO and SAM are not as consistent over time in the western WS, Amundsen Sea, and eastern RS regions (Stammerjohn et al., 2008). As mentioned above, the SIE trend reversed in 2014, and the trend during 1979–2017 was only 50% of that during 1979–2014 (Parkinson, 2019). Sea ice is affected by both thermodynamic and dynamic processes, such as radiation, which can melt ice, and the Antarctic circumpolar current (ACC), which may provide strong sea ice transport (Wu et al., 2020).

In this study, which was motivated by the Antarctic SIE reversed in 2014 (Parkinson, 2019), we focus on the SIE change before and after 2014, and discuss the changes in radiation and energy exchange between the mid-latitudes and the Antarctic that resulted in decreased sea ice in recent years. This study first briefly describes the variation in Antarctic sea ice and then analyzes the causes of its recent features. Moreover, a comparison is performed between the decrease in Antarctic sea ice in recent years and the increase in terms of long-term change, even under warming conditions. Section 2 describes both the SIC and atmospheric data. Section 3 analyzes the sea ice data to describe the basic features from 1979 to 2019 and the characteristics in recent years since 2014. The related atmospheric factors are then discussed in Section 4. Finally, the conclusions are summarized.

2 Data

This study uses satellite data and atmospheric reanalysis products from 1979–2019. The monthly Antarctic SIC data are obtained from the National Snow and Ice Data Center (NSIDC) in Boulder, Colorado, USA. The applied data set is a merged product based on the data of the SMMR (Scanning Multichannel Microwave Radiometer), SSM/I (Special Sensor Microwave/Imager), and SSMIS (Special Sensor Microwave Imager/Sounder) passive microwave sensors processed with the NASA Team algorithm, and it has a spatial resolution of 25 km×25 km (Cavalieri et al., 1996). The SIC accuracy is approximately 5% in winter and 15% in summer (Cavalieri et al., 1992). SIE is defined as the sum of the area of the grid with an SIC of at least 15%, and the SIA is defined as the sum of the SIC times the grid box area for the grid with an SIC of at least 15% (Schlosser et al., 2017). The European Centre for Medium-Range Weather Forecasts (ECMWF) fifth generation (ERA5) dataset is used to investigate the atmospheric conditions, which are available since 1979 (Dee et al., 2011). ERA5 is the fifth generation ECMWF reanalysis for global climate and weather over the past 4–7 decades. Currently, data are available since 1979. The reanalysis combines observations into globally complete fields using the laws of physics via the data assimilation method, which based on observation fields, and a four-dimensional variational assimilation system (4D-VAR) with an integrated spectral model (Hersbach et al., 2020). The spatial resolution of ERA5 is 0.25°×0.25°. The 2 m air temperature ($T_{a\text{-}2m}$), 10 m zonal and meridional wind speeds, cloud fraction, net longwave radiation, downward and net solar radiation, vertical integral northward total energy flux, and northward kinetic energy flux were derived from daily mean values.

3 Temporal evolution of Antarctic sea ice

The monthly averaged SIC and SIE in the Southern Hemisphere and five subregions, namely, the WS, IO, western Pacific Ocean (PO), RS, and BA according to Cavalieri and Parkinson (2008), are analyzed (Fig. 1). The trend of monthly mean SIC from January 1979 to December 2019 (Fig. 2a) and the trend in recent years from January 2014 to December 2019 (Fig. 2b) show opposite results (Fig. 2) and all pass the 95% confidence test. The long-term trend (1979–2019) shows an increase in SIC around the Antarctic continent at a rate of ~2% per decade south of the WS and west of the RS but a decreasing trend with a maximum rate of 6% per decade in the BA and east of the RS. A remarkably negative trend with a rate of ~7%/a is observed in recent years (2014–2019) over in almost the whole WS region, the eastern coastal regions in the IO, the western coastal regions in the PO, and most of the RS region. The negative trend indicates an accelerated decrease in the SIC in these regions. Compared with the negative trend from 1979 to 2019 shown in Fig. 2a, the SIC demonstrated a slight increase off the coastline areas in the BA region (Fig. 2b).

The trends of SIE in the Antarctic and the five subregions from 1979 to 2019 (Fig. 3) have a similar rate as that reported by Parkinson (2019) using the monthly SIE anomaly. Compared with the trend from 1979 to 2013, the long-term trend (1979 to

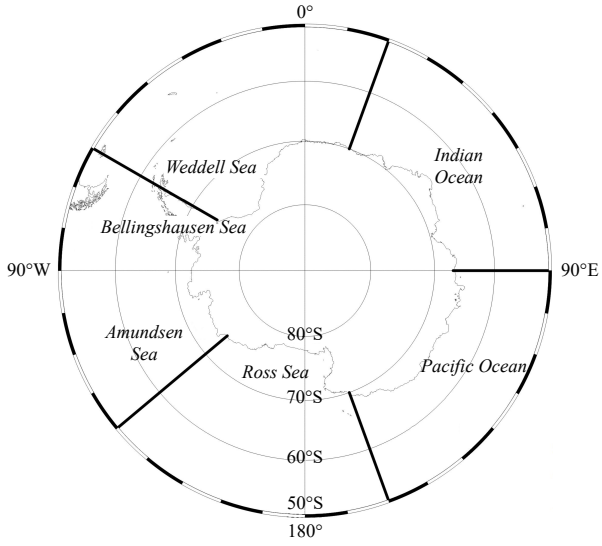

Fig. 1. Location of the five subregions used for the sea ice analyses.

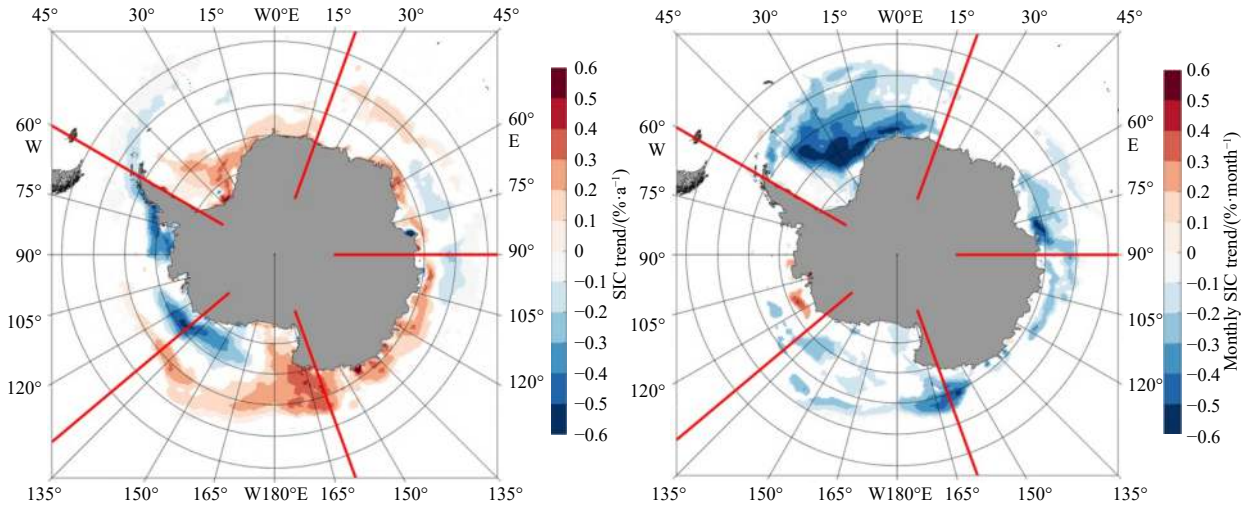

Fig. 2. Yearly SIC trend during January 1979 to December 2019 calculated by monthly SIC anomoly (a) and monthly SIC trend during January 2014 to January 2019 (b). The shading indicates the 95% significance level.

2019) is still positive but shows a slowdown in the Antarctic and its subregions except for the BA region, where a negative trend is observed. However, all the regions show negative trends with decreasing SIE in recent years since 2014. The highest positive SIE rate is observed in the RS region among the five subregions, with a value of (4 636±1 173) km²/a ((1.6±0.4)% per decade) from 1979 to 2019 and a value of (11 584±1 372) km²/a ((4.0±0.5)% per decade) from 1979 to 2013. Furthermore, the SIE has decreased rapidly since 2014 at a rate of (–7 863±1 606) km² per month, which follows the decreasing rate of (16 751±2 104) km² per month observed in the WS region. The trend is the smallest in the BA region among the five subregions, although an accelerated decrease in SIE has also been demonstrated in recent years (2014–2019) with a rate of (–1 733±1 417) km² per month. The seasonal trends of SIE in summer (January–March), autumn (April–June), winter (July–September) and spring (October–December) according to Cavalieri and Parkinson (2008) are shown in Table 1 for the different periods (1979–2019, 1979–2014 and 2014–2019). This table demonstrates that the most remarkable decrease occurs in summer and autumn in the WS and RS regions. The variation in sea ice demonstrates regionally dependent features. The seasonally averaged atmospheric factors that influence sea ice variations are analyzed in the next section.

4 Atmospheric factors

4.1 *Warming air temperature*

A previous study showed that the sea ice decrease in the BA region and increase around in most the rest of the regions can be tied to warming in the regions with decreases and cooling in the regions with increases (Vaughan et al., 2003). However, Antarctic sea ice is increasing under warm atmospheric conditions, which demonstrates a complicated relationship between Antarctic sea ice and $T_{a\text{-}2m}$, where a cooling (warming) surface air temperature trend is associated with an increased (decreased) SIC trend and regional features (Shu et al., 2012).

The $T_{a\text{-}2m}$ trends for the long-term (1979–2019) and short-term (2014–2019) periods show different trends in different regions. The long-term trend (1979–2019) of $T_{a\text{-}2m}$ (Figs 4a and c) shows a slightly negative trend in most of the regions, but a positive trend north of the WS in autumn and west of the Antarctic Peninsula in the Bellingshausen Sea region in summer and autumn. The trend of recent years (2014–2019) shows accelerated warming, especially in summer (Fig. 4b) and autumn (Fig. 4d) in the WS and RS regions. The warming is more robust in autumn and expanded to the WS, IO, PO, and RS regions at a rate of more than 0.6 K/a. The warmer regions coincide with regions with decreased SIC in recent years (Fig. 2b), especially in autumn. The results indicate that the decrease in sea ice in the WS and RS regions is associated with the warming of the $T_{a\text{-}2m}$. Warmer $T_{a\text{-}2m}$ conditions contributed to enhanced sea ice melting in the WS region and portions of the RS region in summer, and it also delayed freezing in autumn in the WS, RS, and parts of the IO and PO regions, resulting in the negative SIC trend (Fig. 2b).

4.2 *Wind anomaly and southward energy*

The $T_{a\text{-}2m}$ and 10 m wind vector differences, which are calculated based on the average value of 2014–2019 minus the average value of 1979–2013, are shown for summer (Fig. 5a), autumn (Fig. 5b), winter (Fig. 5c), and spring (Fig. 5d). The difference fields of the $T_{a\text{-}2m}$ and wind vector exhibit seasonal and regional characteristics. The difference fields reveal warming anomalies and southward wind vectors in winter in the WS, RS and IO and parts of the PO region (Fig. 5c) during 2014–2019, which coincide with the regions of negative SIC trends in recent years (2014–2019) as shown in Fig. 2b. However, the results demonstrate cold anomalies and northward winds in other regions in autumn and winter. The warming anomaly occurs in the RS region in summer and winter but is modest in the RS region in spring during 2014–2019. The warming winter and the southward wind anomaly promoted winter sea ice retreat from 2014–2019.

The vertically integrated southward flux of moist static energy (the sum of dry static energy and latent heat) (Kjellsson et al., 2014), which acts to redistribute energy from warm regions to cold regions, is calculated by subtracting the kinetic energy flux from the total energy flux obtained from the ERA5 dataset. The differences in the vertically integrated southward transport of moist static energy between the period of 2014–2019 and the period of 1979–2013 are shown in Fig. 6. The difference fields of southward energy transport are positive in summer and spring, and negative in autumn and winter in the WS region during

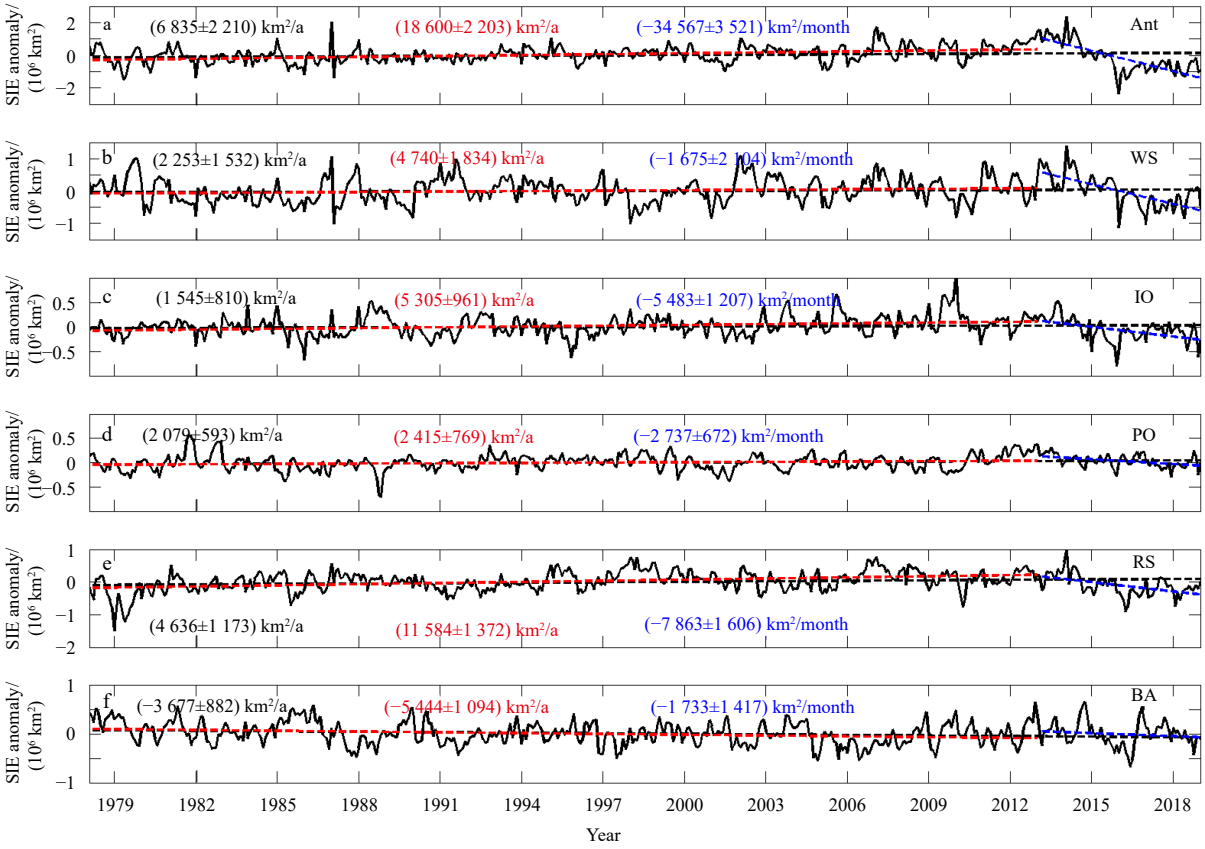

Fig. 3. Monthly trends of SIE during January 1979 to December 2019 (black line), January 1979 to December 2013 (red line) and January 2014 to December 2019 (blue line) for the Antarctic (Ant, a), Weddell Sea (WS, b), Indian Ocean (IO, c), western Pacific Ocean (PO, d), Ross Sea (RS, e), and Bellingshausen Sea and Amundsen Sea (BA, f). The numbers indicate the slope and standard deviations of the yearly trend during the longtime periods (black and red) and monthly trend (blue) for the rencent year in the five subregions.

Table 1. The seasonal trend of SIE in summer (January–March), autumn (April–June), winter (July–September) and spring (October–December)

Period	Sector	Yearly SIE trend		Seasonal trend of SIE							
				Summer (JFM)		Autumn (AMJ)		Winter (JAS)		Spring (OND)	
		Value/ (10^3 km²·a^{-1})	*R*	Value/ (10^3 km²·a^{-1})	*R*	Value/ (10^3 km²·a^{-1})	*R*	Value/ (10^3 km²·a^{-1})	*R*	Value/ (10^3 km²·a^{-1})	*R*
1979–2019	Ant	6.8±2.2	**3.1**	7.2±7.7	0.9	10.4±8.1	1.3	8.2±4.7	1.7	1.5±6.8	0.2
	WS	2.3±1.5	1.5	12.7±4.9	**2.6**	4.8±4.8	1.0	−3.3±4.2	0.8	−5.2±4.9	1.1
	IO	1.5±0.8	1.9	2.2±1.3	1.7	2.6±2.1	1.3	1.7±2.8	0.6	−0.3±3.2	0.1
	PO	2.1±0.6	**3.5**	3.1±1.5	**2.1**	3.1±1.5	**2.1**	1.6±2.2	0.7	0.5±1.9	0.3
	RS	4.6±1.2	**4.0**	−1.2±4.1	0.3	6.9±3.7	1.9	5.4±3.2	1.7	7.5±3.6	**2.1**
	BA	−3.7±0.9	**4.2**	−9.5±1.8	**5.3**	−7.1±2.5	**2.8**	2.8±2.9	1.0	−0.9±3.2	0.3
1979–2013	Ant	18.6±2.2	**8.4**	15.8±7.7	**2.1**	21.5±7.4	**2.9**	17.3±4.3	**4.0**	19.6±5.9	**3.3**
	WS	4.7±1.8	**2.6**	14.9±5.6	**2.7**	8.2±5.3	1.5	−3.4±5.4	0.6	−1.0±6.1	0.2
	IO	5.3±1.0	**5.5**	2.8±1.6	1.8	5.6±2.6	**2.2**	6.4±3.2	2.0	6.3±3.6	1.7
	PO	2.4±0.8	**3.1**	3.2±2.0	1.6	3.9±1.8	**2.1**	1.0±2.9	0.3	1.6±2.5	0.6
	RS	11.6±1.4	**8.4**	7.3±4.6	1.6	12.3±4.4	**2.8**	12.0±3.8	**3.2**	14.9±4.3	**3.4**
	BA	−5.4±1.1	**5.0**	−12.4±2.2	**5.5**	−8.5±3.0	**2.8**	1.2±3.5	0.4	−2.1±4.2	0.5
2014–2019	Ant	−414.8±42.2	**9.8**	−396.3±114.3	**3.5**	−449.6±118	**3.8**	−279.6±68.1	**4.1**	−341.8±131.6	2.6
	WS	−201.0±25.3	**8.0**	−208.4±62.5	**3.3**	−192.7±67.8	**2.8**	−22.8±59.9	0.4	−101.5±63.8	1.6
	IO	−65.8±14.5	**4.5**	−17.3±23.2	0.7	−62.5±12.6	**5.0**	−76.9±42.6	1.8	−68.4±47.9	1.4
	PO	−32.9±8.1	**4.1**	−50.5±13.3	**3.8**	−59.0±6.7	**8.8**	−26.1±26.2	1.0	−46.1±29.1	1.6
	RS	−94.4±19.3	**4.9**	−151.9±47.2	**3.2**	−123.6±36.9	**3.3**	−84.7±39.1	2.2	−71.6±35.3	2.0
	BA	−20.8±17.0	1.2	31.8±19.1	1.7	−11.7±46.6	0.3	−69.1±47.5	1.5	−54.3±46.9	1.2

Note: *R* is the ratio of the slope magnitude to its standard deviation. The bold numbers indicate the 95% significance level.

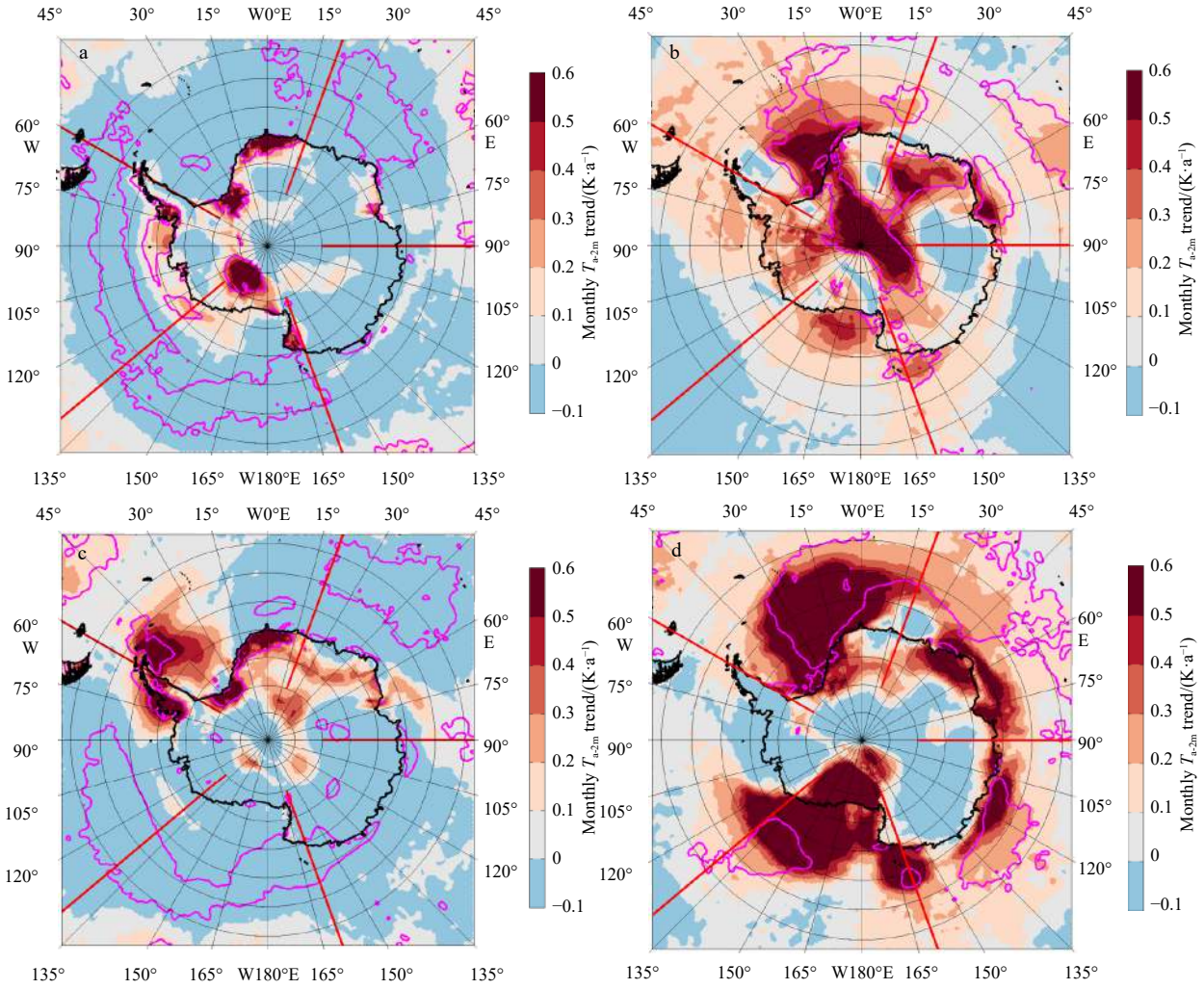

Fig. 4. Monthly $T_{a\text{-}2m}$ trend during January 1979 to December 2019 in summer (a) and autumn (c), and January 2014 to December 2019 in summer (b) and autumn (d). The pink contours indicate the 90% significance level.

2014–2019. The increased southward energy transport in summer and spring could transport warmer air from the north, which can cause warming in the WS region, as shown by the $T_{a\text{-}2m}$ trend (Fig. 4b), thereby promoting enhanced ice melting, especially early melt onset in spring from 2014–2019. The southward transport of moist static energy shows increases in the western RS and eastern PO regions during all seasons (Fig. 6) in the 2014–2019 period, which coincides with the wind anomaly (Fig. 5) and favors the sea ice decrease in the RS region.

4.3 *Cloudiness and radiation*

Increasing cloud cover can warm the surface, which helps reduce ice. Previous results show that the negative cloud fraction anomalies in winter can play a vital role in the following summer sea ice distribution, which results in a negative surface radiation budget and cooling of the surface and promotes more sea ice growth (Wang et al., 2019). ERA-Interim monthly mean cloud fraction matched the observations within 5% in the Southern Ocean (Naud et al., 2014). ERA5 is the new version of the ECMWF reanalysis, and clouds over the ocean are ~10% smaller in ERA5 than in MODIS dataset (Yao et al., 2020). Great differences in cloud cover occur in the sea regions around the Antarctic continent. In the western RS and eastern PO regions, the cloudiness difference fields of 2014–2019 minus 1979–2013 show more cloudiness in autumn, winter and spring (Figs 7b, c and d). This increased cloud cover means more downward longwave radiation, which coincides with the regions with reduced sea ice since 2014. In the WS region, however, the cloudiness difference fields of 2014–2019 minus 1979–2013 demonstrate less cloudiness in all seasons, which does not favor the sea ice decrease. The clouds show obvious regional features and play an important role in the sea ice decrease in the western RS and eastern PO regions. However, the cloud fraction is not the controlling factor for sea ice in the RS region.

Previous results show that downward longwave radiation was the main factor controlling recent sea ice melting in the Arctic (Francis and Hunter, 2006; Kapsch et al., 2013). The surface net downward longwave flux demonstrates remarkable negative differences in the WS region in summer and autumn (Fig. 8) during 2014–2019, which coincided with the cloud difference (Figs 7b and c). The reduction in cloud cover resulted in less net downward longwave radiation and more downward solar radiation (Fig. 8). In the western RS and eastern PO regions, greater net downward longwave flux occurred in spring in association with the increased cloudiness during 2014–2019, which was not beneficial for increased sea ice in the following summer. A greater amount of net downward longwave flux can prevent ice freezing

in autumn and advance the onset of the melting in spring or summer.

The surface downward solar radiation increased in summer (Fig. 9a) and was indistinct or slightly negative in spring in the WS region (Fig. 9b). The net downward solar radiation showed a more notable increase in spring (Fig. 10b) during 2014–2019,

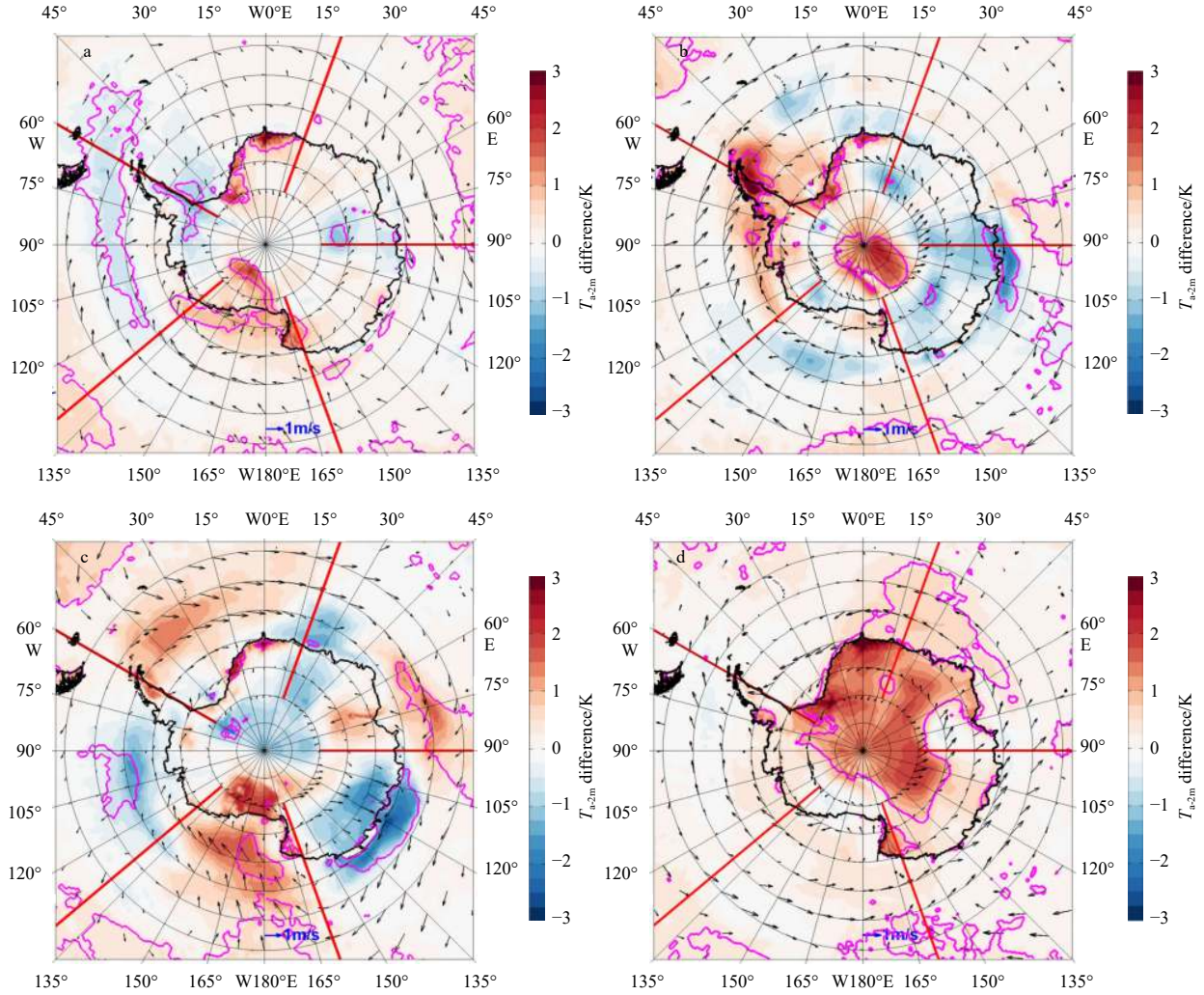

Fig. 5. Distribution of $T_{a\text{-}2m}$ differences (shading) and 10 m wind differences (vector) (2014–2019 minus 1979–2013) in summer (a), autumn (b), winter (c), and spring (d). The pink contours indicate the 90% significance level.

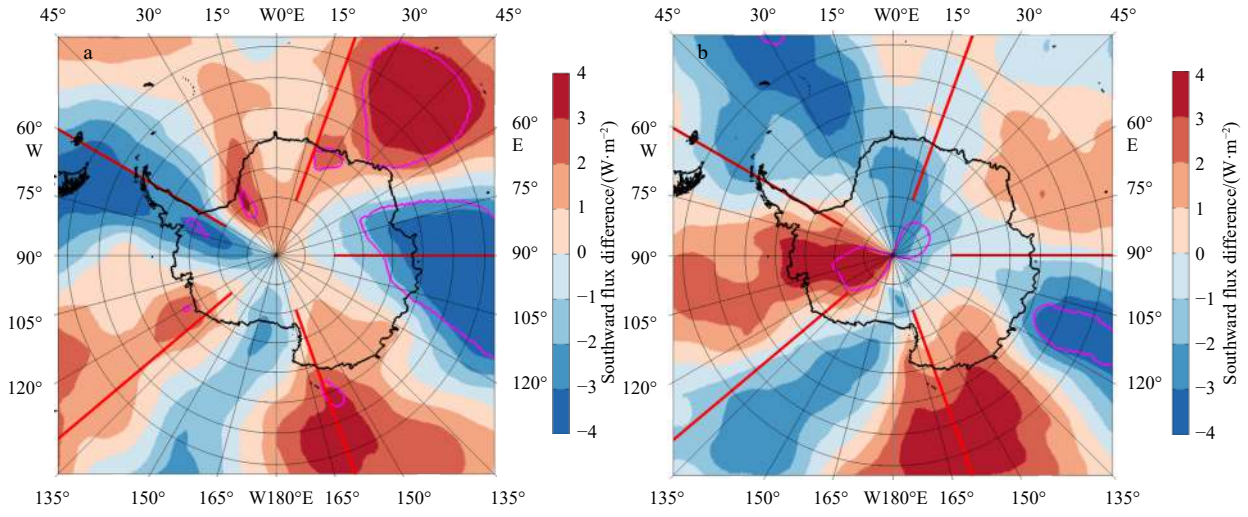

Fig. 6.

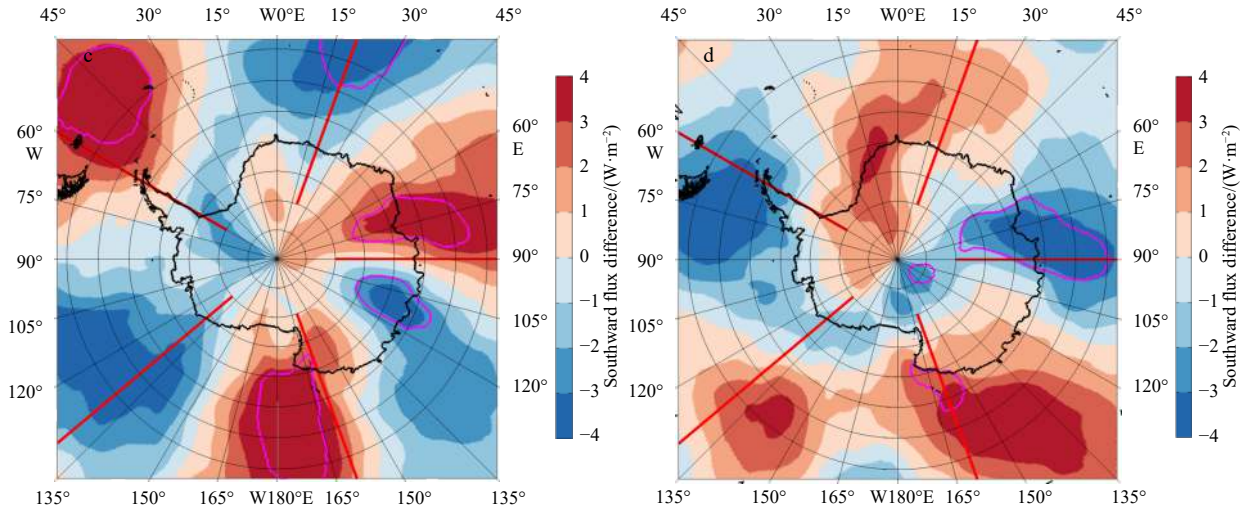

Fig. 6. Distribution of the vertically integrated southward flux difference of moist static energy (2014–2019 minus 1979–2013) in summer (a), autumn (b), winter (c), and spring (d). The pink contours indicate the 90% significance level.

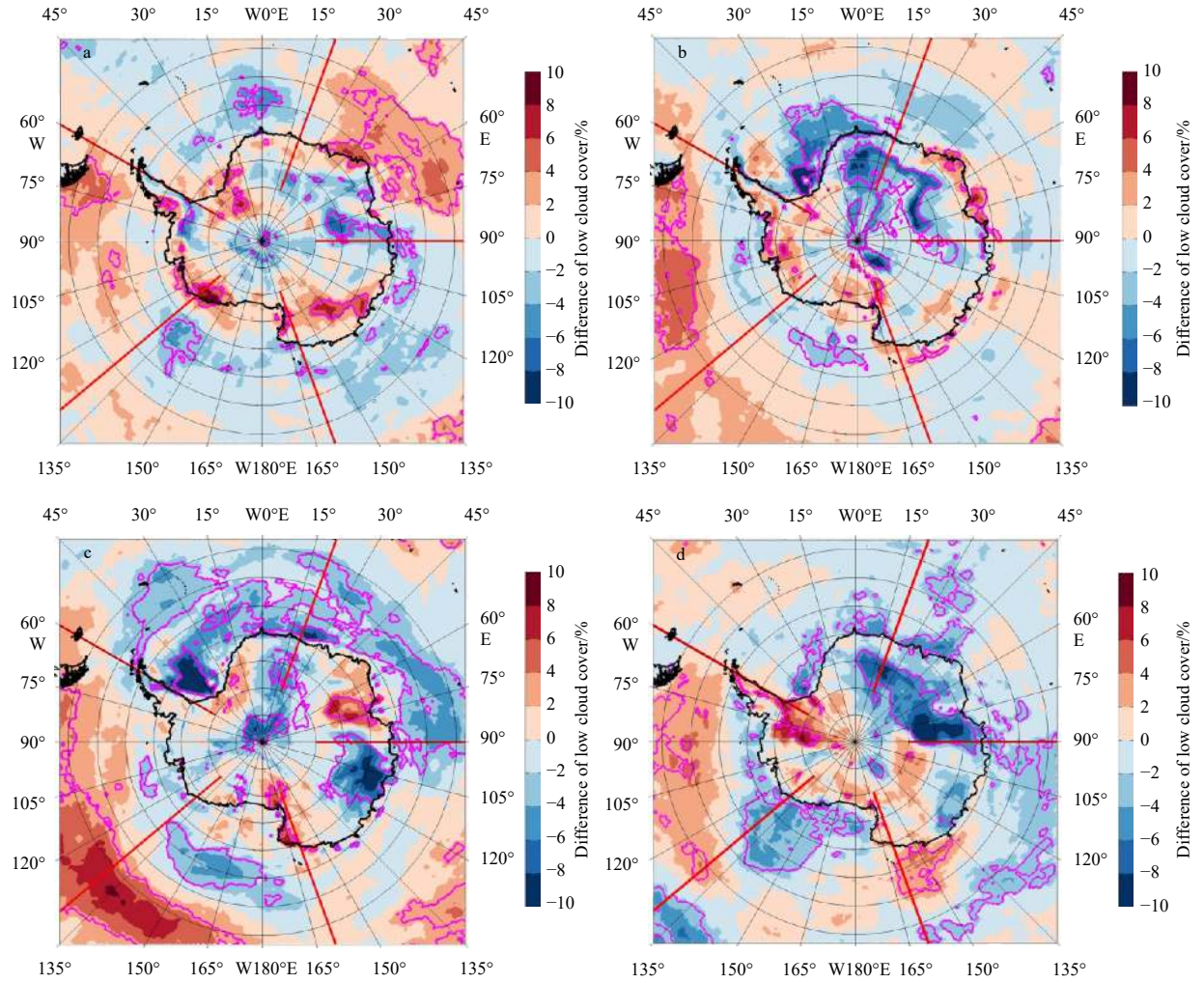

Fig. 7. Distribution of low cloud cover difference (2014–2019 minus 1979–2013) in summer (a), autumn (b), winter (c), and spring (d). The pink contours indicate the 90% significance level.

which means less sea ice and reduced surface reflection in spring. The local warming results from the enhanced absorption of solar radiation in summer, resulting in more ice melting and delayed freezing in autumn in the WS region. The early melting in spring and the southward energy transport also contributed to the reduced sea ice in summer and spring, which favored the sea

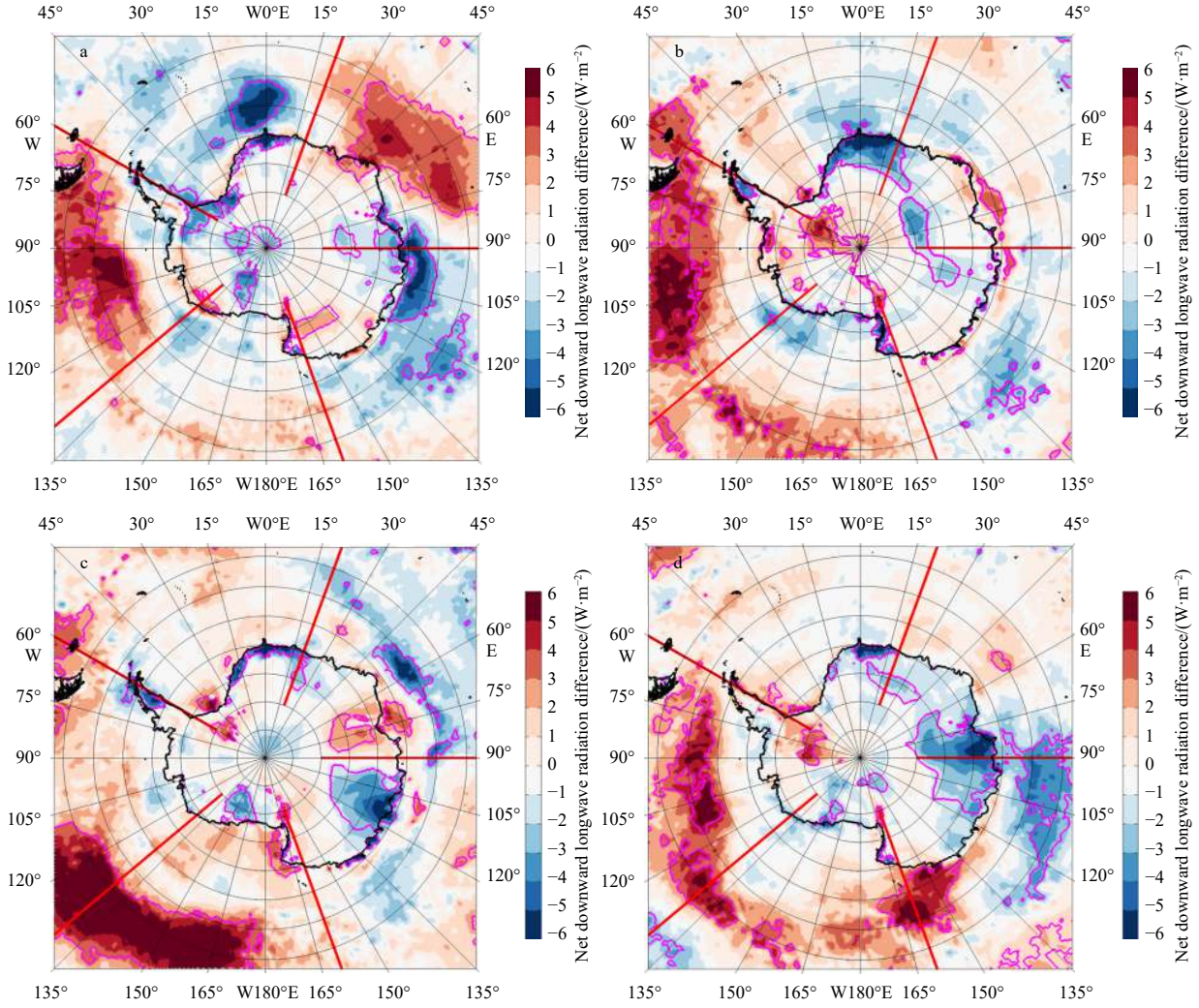

Fig. 8. The distribution of net downward longwave radiation difference (2014–2019 minus 1979–2013) in summer (a), autumn (b), winter (c), and spring (d). The pink contours indicate the 90% significance level.

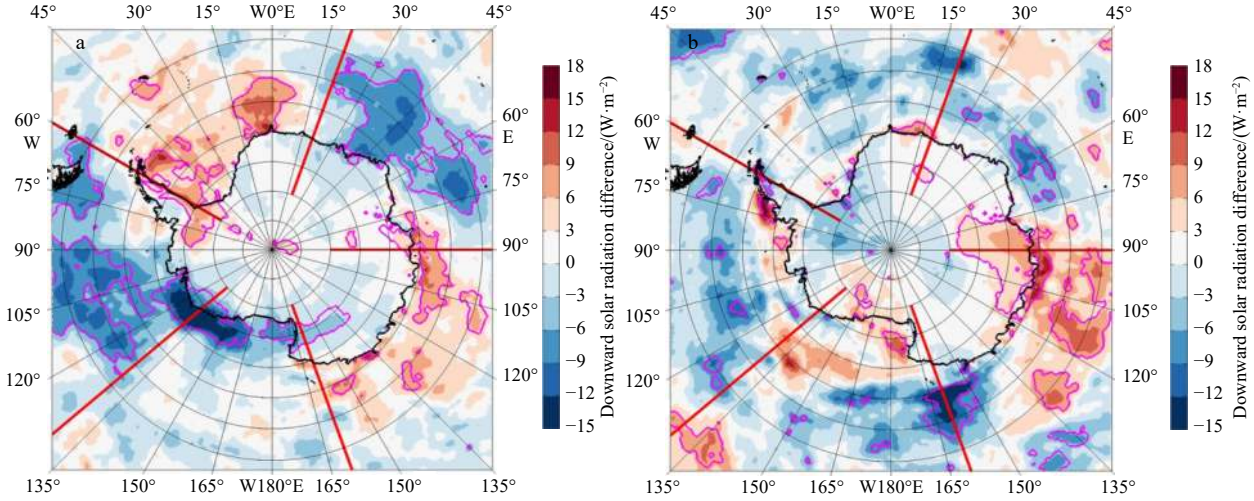

Fig. 9. The distribution of downward solar radiation difference (2014–2019 minus 1979–2013) in summer (a) and spring (b). The pink contours indicate the 90% significance level.

ice decrease in the WS region. The net downward solar radiation increases in part of the PO region in summer and spring. The main factor contributing to the sea ice decrease in the RS region is southward energy transport in nearly all seasons, which results

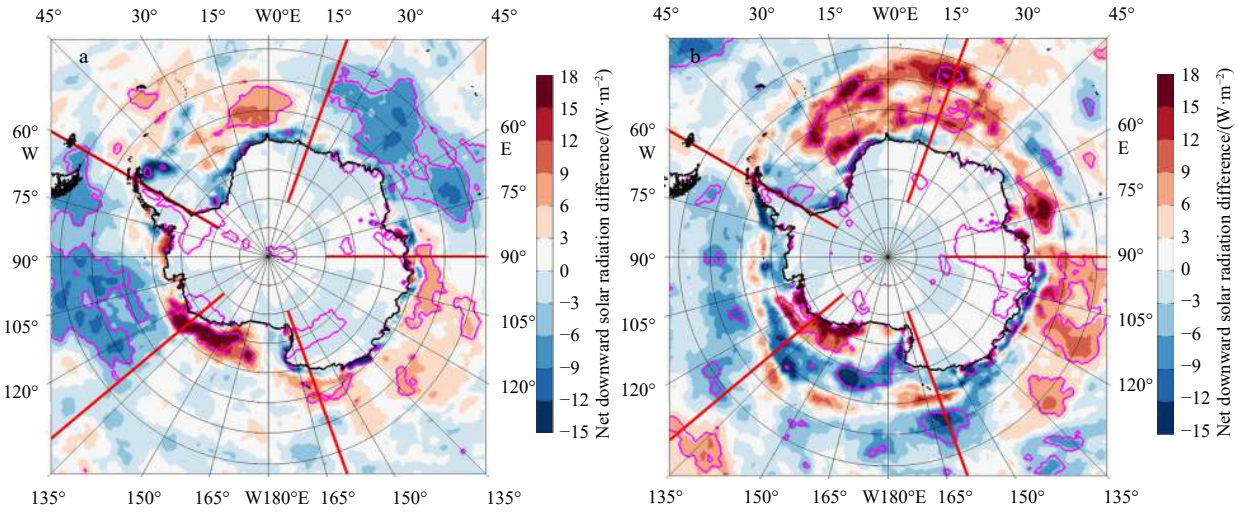

Fig. 10. The distribution of net downward solar radiation difference (2014–2019 minus 1979–2013) in summer (a) and spring (b). The pink contours indicate the 90% significance level.

in warming and more net longwave radiation in the cold seasons.

5 Conclusions

The spatial and temporal evolution of SIC based on monthly passive microwave sensor data from 1979 to 2019 are analyzed in this study. The analysis used Antarctic SIC data collected over 40 years, and the results of this study show trends that are similar to those identified by Parkinson (2019) but differ from those identified by other studies (Cavalieri and Parkinson, 2008; Parkinson and Cavalieri, 2012; Shu et al., 2012). The current study also analyzes the related atmospheric factors that influence the variation in SIC to assess the causes of the decreasing or decelerating SIC and SIE in recent years (2014–2019) compared with those in in previous decades (1979–2013).

The results demonstrate that Antarctic SIE has increased over the past 40 years from 1979 to 2019, although the rate of the positive trend of Antarctic SIE decelerated over the past decade and has become negative in recent years. Remarkable decreases in SIC have occurred in the WS, RS, and parts of the IO and PO regions. In the long-term series (1979–2019), the most obvious positive SIC trends are observed in the WS, IO, PO, and RS regions while a negative trend is observed in the BA region. The most obvious negative trends in recent years are observed in the WS and RS regions. The trend of Antarctic SIE decreased from (1.5±0.2)% per decade from 1979–2013 to (0.6±0.2)% per decade during 1979–2019. Antarctic sea ice has decreased in recent years (2014–2019) at a rate of (415±42.3)×10^3 km^2/a compared with the long-term positive trend, and regional characteristics are observed.

In recent years, the decreases in SIC and SIE have been regionally dependent on different causes. The trend of $T_{a\text{-}2m}$ is correlated with the trend of SIC in regions where the SIC has recently decreased, especially in the WS and RS regions. A previous study demonstrated that a cooling (warming) surface air temperature trend is associated with an positive (negative) SIC trend in the Antarctic (Shu et al., 2012). However, in recent years, the continued warming trend has been associated with a decreasing SIC trend in the Antarctic. The effect of atmospheric factors also demonstrated regional characteristics. In the WS region, local warming caused by fewer clouds cloud results in more absorbed solar energy in summer, which favors sea ice melting and results in less ice and delayed freezing in autumn. The reduced amount of ice also results in more absorbed solar radiation in spring, which favors early melting. Thus, this positive feedback plays a leading role in the reduction of sea ice in the WS region. The more southward transport of energy also contributes to the sea ice reduction. In the RS region, the increased southward transport in all seasons and the greater net longwave radiation associated with increased cloudiness play important roles in the sea ice decrease, and these are different from the local positive feedback in the WS region. The greater cloud cover and net longwave radiation in winter and spring can prevent ice growth, which makes the ice more prone to melting or the impacts of dynamic processes. The results show that the reasons for the decreases in SIC and SIE in recent years are different in different subregions. The more absorbed solar radiation and southward transported energy contribute to the continual warming conditions, especially the warming in summer and autumn in recent years compared with the long-term trend, which thereby reducing the SIC and SIE decrease.

Acknowledgements

SIC data are provided by NSIDC (http://nsidc.org/data/nsidc-0051.html). ERA5 data are from https://cds.climate.copernicus.eu/#!/search?text=ERA5&type=dataset/. We thank Ray Miller for editing the English language.

References

Bromwich D H, Nicolas J P, Monaghan A J, et al. 2013. Central West Antarctica among the most rapidly warming regions on Earth. Nature Geoscience, 6(2): 139–145, doi: 10.1038/NGEO1671

Cavalieri D J, Crawford J, Drinkwater M, et al. 1992. NASA sea ice validation program for the DMSP SSM/I: final report. NASA Technical Memorandum 104559. Washington, DC: National Aeronautics and Space Administration

Cavalieri D J, Gloersen P, Parkinson C L, et al. 1997. Observed hemispheric asymmetry in global sea ice changes. Science, 278(5340): 1104–1106, doi: 10.1126/science.278.5340.1104

Cavalieri D J, Parkinson C L. 2008. Antarctic sea ice variability and trends, 1979–2006. Journal of Geophysical Research: Oceans, 113(C7): C07004, doi: 10.1029/2007JC004564

Cavalieri D J, Parkinson L C, Gloersen P, et al. 1996. Sea ice concentrations from Nimbus-7 SMMR and DMSP SSM/I-SSMIS passive microwave data, Version 1. [Antarctic, 1979 to 2019]. Boulder, Colorado USA: NASA National Snow and Ice Data

Center Distributed Active Archive Center, doi: https://doi.org/10.5067/8GQ8LZQVL0VL
Cerrone D, Fusco G. 2018. Low-frequency climate modes and Antarctic sea ice variations, 1982–2013. Journal of Climate, 31(1): 147–175, doi: 10.1175/JCLI-D-17-0184.1
Comiso J C, Gersten R A, Stock L V, et al. 2017a. Positive trend in the Antarctic sea ice cover and associated changes in surface temperature. Journal of Climate, 30(6): 2251–2267, doi: 10.1175/JCLI-D-16-0408.1
Comiso J C, Meier W N, Gersten R. 2017b. Variability and trends in the Arctic Sea ice cover: results from different techniques. Journal of Geophysical Research: Oceans, 122(8): 6883–6900, doi: 10.1002/2017JC012768
Comiso J C, Nishio F. 2008. Trends in the sea ice cover using enhanced and compatible AMSR-E, SSM/I, and SMMR data. Journal of Geophysical Research: Oceans, 113(C2): C02S07, doi: 10.1029/2007JC004257
Curry J A, Schramm J L, Ebert E E. 1995. Sea ice-albedo climate feedback mechanism. Journal of Climate, 8(2): 240–247, doi: 10.1175/1520-0442(1995)008<0240:SIACFM>2.0.CO;2
Dee D P, Uppala S M, Simmons A J, et al. 2011. The ERA-Interim reanalysis: configuration and performance of the data assimilation system. Quarterly Journal of the Royal Meteorological Society, 137(656): 553–597, doi: 10.1002/qj.828
Doddridge E W, Marshall J. 2017. Modulation of the seasonal cycle of Antarctic sea ice extent related to the southern annular mode. Geophysical Research Letters, 44(19): 9761–9768, doi: 10.1002/2017GL074319
Elders A, Pegion K. 2019. Diagnosing sea ice from the north American multi model ensemble and implications on mid-latitude winter climate. Climate Dynamics, 53(12): 7237–7250, doi: 10.1007/s00382-017-4049-3
Francis J A, Hunter E. 2006. New insight into the disappearing Arctic sea ice. Eos, Transactions American Geophysical Union, 87(46): 509–511, doi: 10.1029/2006EO460001
Hersbach H, Bell B, Berrisford P, et al. 2020. The ERA5 global reanalysis. Quarterly Journal of the Royal Meteorological Society, 146(730): 1999–2049, doi: 10.1002/qj.3803
Holland M M, Landrum L, Kostov Y, et al. 2017. Sensitivity of Antarctic sea ice to the Southern Annular Mode in coupled climate models. Climate Dynamics, 49(5): 1813–1831, doi: 10.1007/s00382-016-3424-9
Kapsch M L, Graversen R G, Tjernström M. 2013. Springtime atmospheric energy transport and the control of Arctic summer sea-ice extent. Nature Climate Change, 3(8): 744–748, doi: 10.1038/nclimate1884
Kjellsson J, Döös K, Laliberté F B, et al. 2014. The atmospheric general circulation in thermodynamical coordinates. Journal of the Atmospheric Sciences, 71(3): 916–928, doi: 10.1175/JAS-D-13-0173.1
Lee S K, Volkov D L, Lopez H, et al. 2017. Wind-driven ocean dynamics impact on the contrasting sea-ice trends around West Antarctica. Journal of Geophysical Research: Oceans, 122(5): 4413–4430, doi: 10.1002/2016JC012416
Liu Jiping, Curry J A, Martinson D G. 2004. Interpretation of recent Antarctic sea ice variability. Geophysical Research Letters, 31(2): L02205, doi: 10.1029/2003GL018732
Marshall G J. 2003. Trends in the southern annular mode from observations and reanalyses. Journal of Climate, 16(24): 4134–4143, doi: 10.1175/1520-0442(2003)016<4134:TITSAM>2.0.CO;2
Marshall G J. 2007. Half-century seasonal relationships between the southern annular mode and Antarctic temperatures. International Journal of Climatology, 27(3): 373–383, doi: 10.1002/joc.1407
Meehl G A, Arblaster J M, Chung C T Y, et al. 2019. Sustained ocean changes contributed to sudden Antarctic sea ice retreat in late 2016. Nature Communications, 10(1): 14, doi: 10.1038/s41467-018-07865-9
Naud C M, Booth J F, Del Genio A D, et al. 2014. Evaluation of ERA-Interim and MERRA cloudiness in the Southern Ocean. Journal of Climate, 27(5): 2109–2124, doi: 10.1175/JCLI-D-13-00432.1
Nicolas J P, Bromwich D H. 2014. New reconstruction of Antarctic near-surface temperatures: multidecadal trends and reliability of global reanalyses. Journal of Climate, 27(21): 8070–8093, doi: 10.1175/JCLI-D-13-00733.1
Parkinson C L, Cavalieri D J. 2012. Antarctic sea ice variability and trends, 1979–2010. The Cryosphere, 6(4): 871–880, doi: 10.5194/tc-6-871-2012
Parkinson C L. 2019. A 40-y record reveals gradual Antarctic sea ice increases followed by decreases at rates far exceeding the rates seen in the Arctic. Proceedings of the National Academy of Sciences of the United States of America, 116(29): 14414–14423, doi: 10.1073/pnas.1906556116
Schlosser E, Haumann F A, Raphael M N. 2017. Atmospheric influences on the anomalous 2016 Antarctic sea ice decay. The Cryosphere, 12(3): 1103–1119, doi: 10.5194/tc-12-1103-2018
Shu Qi, Qiao Fangli, Song Zhenya, et al. 2012. Sea ice trends in the Antarctic and their relationship to surface air temperature during 1979–2009. Climate Dynamics, 38(11): 2355–2363, doi: 10.1007/s00382-011-1143-9
Simpkins G R, Ciasto L M, England M H. 2013. Observed variations in multidecadal Antarctic sea ice trends during 1979–2012. Geophysical Research Letters, 40(14): 3643–3648, doi: 10.1002/grl.50715
Stammerjohn S E, Martinson D G, Smith R C, et al. 2008. Trends in Antarctic annual sea ice retreat and advance and their relation to El Niño-Southern Oscillation and Southern Annular Mode variability. Journal of Geophysical Research: Oceans, 113(C3): C03S90, doi: 10.1029/2007JC004269
Stuecker M F, Bitz C M, Armour K C, et al. 2017. Conditions leading to the unprecedented low Antarctic sea ice extent during the 2016 austral spring season. Geophysical Research Letters, 44(17): 9008–9019, doi: 10.1002/2017GL074691
Thompson D W J, Wallace J M. 2000. Annular modes in the extratropical circulation. part I: month-to-month variability. Journal of Climate, 13(5): 1000–1016, doi: 10.1175/1520-0442(2000)013<1000:AMITEC>2.0.CO;2
Turner J, Phillips T, Marshall G J, et al. 2017. Unprecedented springtime retreat of Antarctic sea ice in 2016. Geophysical Research Letters, 44(13): 6868–6875, doi: 10.1002/2017GL073656
Vaughan D G, Marshall G J, Connolley W M, et al. 2003. Recent rapid regional climate warming on the Antarctic peninsula. Climatic Change, 60(3): 243–274, doi: 10.1023/A:1026021217991
Wang Guomin, Hendon H H, Arblaster J M, et al. 2019. Compounding tropical and stratospheric forcing of the record low Antarctic sea-ice in 2016. Nature Communications, 10(1): 13, doi: 10.1038/s41467-018-07689-7
Wu Yang, Wang Zhaomin, Liu Chengyan, et al. 2020. Impacts of high-frequency atmospheric forcing on Southern Ocean circulation and Antarctic sea ice. Advances in Atmospheric Sciences, 37(5): 515–531, doi: 10.1007/s00376-020-9203-x
Yao Bin, Teng Shiwen, Lai Ruize, et al. 2020. Can atmospheric reanalyses (CRA and ERA5) represent cloud spatiotemporal characteristics?. Atmospheric Research, 244: 105091, doi: 10.1016/j.atmosres.2020.105091
Yuan Naiming, Ding Minghu, Ludescher J, et al. 2017. Increase of the Antarctic Sea Ice Extent is highly significant only in the Ross Sea. Scientific Reports, 7: 41096, doi: 10.1038/srep41096
Zhang Jinlun. 2007. Increasing Antarctic sea ice under warming atmospheric and oceanic conditions. Journal of Climate, 20(11): 2515–2529, doi: 10.1175/JCLI4136.1
Zwally H J, Comiso J C, Parkinson C L, et al. 2002. Variability of Antarctic sea ice 1979–1998. Journal of Geophysical Research: Oceans, 107(C5): 3041, doi: 10.1029/2000JC000733